



Published in final edited form as:

Gene Expr. 2017 February 10; 17(2): 115–127. doi:10.3727/105221616X692991.

Bile Duct Ligation Induces ATZ Globule Clearance In a Mouse Model of Alpha-1 Antitrypsin Deficiency

Zahida Khan, MD, PhD^{1,2,3}, Shinichiro Yokota, MD^{4,5}, Yoshihiro Ono, MD⁴, Aaron W. Bell, PhD², Donna B. Stolz, PhD^{3,5}, and George K. Michalopoulos, MD, PhD^{2,3}

¹Department of Pediatrics, Children's Hospital of Pittsburgh of UPMC, Pittsburgh, PA, USA

²Department of Pathology, University of Pittsburgh School of Medicine, Pittsburgh, PA, USA

³McGowan Institute for Regenerative Medicine, University of Pittsburgh, Pittsburgh, PA, USA

⁴Department of Surgery, University of Pittsburgh School of Medicine, Pittsburgh, PA, USA

⁵Department of Surgery, Jichi Medical University, Japan

⁶Department of Cell Biology, University of Pittsburgh School of Medicine, Pittsburgh, PA, USA

Abstract

Background—Alpha-1 antitrypsin deficiency (A1ATD) can progress to cirrhosis and hepatocellular carcinoma; however, not all patients are susceptible to severe liver disease. In A1ATD, a toxic gain-of-function mutation generates insoluble ATZ “globules” in hepatocytes, overwhelming protein clearance mechanisms. The relationship between bile acids and hepatocytic autophagy is less clear, but may involve altered gene expression pathways. Based on previous findings that bile duct ligation (BDL) induces autophagy, we hypothesized that retained bile acids may have hepatoprotective effects in PiZZ transgenic mice, which model A1ATD.

Methods—We performed BDL and partial BDL (pBDL) in PiZZ mice, followed by analysis of liver tissues.

Results—PiZZ liver subjected to BDL showed up to 50% clearance of ATZ globules, with increased expression of autophagy proteins. Analysis of transcription factors revealed significant changes. Surprisingly nuclear TFEB, a master regulator of autophagy, remained unchanged. pBDL confirmed that ATZ globule clearance was induced by localized stimuli rather than diet or systemic effects. Several genes involved in bile metabolism were over-expressed in globule-devoid hepatocytes, compared to globule-containing cells.

Conclusions—Retained bile acids led to a dramatic reduction of ATZ globules, with enhanced hepatocyte regeneration and autophagy. These findings support investigation of synthetic bile acids as potential autophagy-enhancing agents.

Corresponding author: Zahida Khan, MD PhD, Children's Hospital of Pittsburgh of UPMC, Division of Pediatric Gastroenterology, Hepatology, and Nutrition 4401 Penn Avenue, Faculty Pavilion 6th Floor, Pittsburgh, PA 15224-1334 USA, Office: (412) 692-5180, Fax: (412) 692-7355, zahida.khan@chp.edu.

Disclosures/Conflict of Interest: The authors do not have any disclosures or conflicts of interest.

Keywords

hepatocyte; autophagy; PiZZ; cholestasis; liver regeneration

Introduction

Alpha-1 antitrypsin deficiency (A1ATD) is the most common inherited pediatric liver disorder, and the most frequent genetic cause of liver transplantation (reviewed in¹). The classical form of A1ATD involves homozygosity for the *Z* allele (PiZZ) in the *SERPINA1* gene, causing accumulation of misfolded ATZ protein monomers in the endoplasmic reticulum (ER) of hepatocytes. These toxic insoluble globules are periodic acid–Schiff (PAS)+/diastase-resistant. Chronic hepatocyte injury from ER stress can progress to cirrhosis and hepatocellular carcinoma². Although liver transplantation remains the only cure for patients with severe liver disease, prospective studies in PiZZ newborns found that only ~8% of homozygotes develop clinically significant liver disease by adulthood, suggesting the role of other genetic or environmental modifiers of susceptibility³.

The PiZZ transgenic mouse overexpresses human ATZ protein, providing a useful model to study A1ATD-related liver disease⁴. Histologically, two main hepatocyte populations exist, described as “globule-containing” (GC) or “globule-devoid” (GD)⁵. *In vivo* studies have shown that stressed GC hepatocytes demonstrate decreased proliferation and increased apoptosis compared to healthier GD hepatocytes^{2,6-9}. These differential capabilities can be exploited with autophagy-enhancing agents to promote ATZ globule clearance^{7,10}.

At the transcriptional level, regulation of autophagy is tightly coordinated with induction of nuclear transcription factors¹¹⁻¹³. Nuclear receptor pathways offer promising targets for pharmacologic agonists, such as synthetic bile acids, in treating chronic liver diseases¹⁴. The relationship of bile acids and hepatocytic autophagy is less clear^{15,16}. A recent study found that although bile duct ligation (BDL) led to cholestatic liver injury in mice, activation of autophagy in hepatocytes was protective¹⁵. In human liver, biliary obstruction induces transcriptional reprogramming in hepatocytes¹⁷. Thus, altered gene expression may be a common survival mechanism following BDL. We therefore hypothesized that BDL may also lead to hepatoprotective effects in PiZZ mice. In this study, we show that retained bile acids trigger alternate transcriptional pathways and enhance hepatocyte regeneration and autophagy, leading to ATZ globule clearance.

Materials and Methods

Animal surgeries

We used 3-month old mice, since ATZ globules in PiZZ mouse liver peak at ages 2-3 months. We used male PiZZ (c57/b6) mice, given sex-dependent phenotypic variations. Female PiZZ mice have significantly less ATZ globules compared to male PiZZ mice, making them less suitable for our studies¹⁸. Mice were maintained on 12-hour light/dark cycles, with *ad libidum* mouse chow and water in an approved barrier facility. Surgery was performed under isoflurane anesthesia. The mouse was positioned on the surgical table

under surgical microscopy apparatus, and a midline abdominal incision exposed the hepatic hilum and hepato-duodenal ligament. For total BDL, the common bile duct was dissected from the hepato-duodenal ligament and ligated with 7-0 silk. A double ligature was made. Sham operations for BDL were performed in the same way without bile duct dissection and ligation. For partial BDL (pBDL), the unligated right lobe served as an internal control for the ligated left lobe, subjected to the same systemic effects, such as diet or circulating factors activated by BDL. Previous studies have observed less fibrosis and necrosis in the internal control lobe in pBDL¹⁹. For pBDL, the main biliary confluence of the right and left bile duct was carefully visualized at the hepatic hilum, and only the left bile duct was ligated with 10-0 nylon. The abdominal incision was closed in two layers using a continuous running suture. Liver tissues were harvested at days 3, 7, and 14 after surgery (n = 3-5 mice per time point). All procedures were in accordance with ethical guidelines of the Institutional Animal Care and Use Committee of the University of Pittsburgh (#15035202).

Histology and globule morphometry

Immunohistochemistry and confocal immunofluorescence microscopy were performed as described²⁰. See Table 1 for antibodies. PASD staining was performed according to manufacturer's protocol (Sigma-Aldrich). For quantitative ATZ globule morphometry, formalin-fixed paraffin sections were co-stained with PASD and DAPI nuclear stain, and whole slides of tissue sections from each liver lobe were imaged and reconstructed on a Nikon A1 tiling fluorescence microscope. The % area of ATZ globules per cell nucleus was quantified blindly using an automated algorithm designed with Nikon Elements software.

Western blots

Total cell lysates or nuclear extracts were separated on SDS-PAGE, followed by Western blotting as described²⁰, with antibodies in Table 1.

Laser capture analysis

Frozen unfixed liver tissue sections (n=3) were stained with cresyl violet, and clusters of GC and GD cells were isolated via laser capture microdissection (LCM) for total RNA isolation, as described⁸. Gene array analysis of RNA expression was performed using Affymetrix mouse 2.0 ST arrays.

Results

BDL induces clearance of ATZ globules in PiZZ mouse liver

We performed BDL in PiZZ mice to provide a stimulus for biliary-driven regeneration. Serum biochemistries (Figure 1A) confirmed acute liver injury at day 3, followed by chronic cholestasis at days 7 and 14 after BDL²¹. We observed a remarkable decrease in PASD staining in BDL livers compared to age- and sex-matched sham controls, as early as 3 days after BDL (Figure 1B). We then performed blinded automated globule morphometry of whole tissue sections from multiple liver lobes, and found as high as 50% reduction in ATZ globules compared to sham controls (Figure 1C). This indicates more accelerated globule clearance than expected with aging alone. Interestingly, residual GC cells localized to periportal regions between proliferating intralobular bile ducts (Figure 1D).

BDL induces an early regenerative response in GD hepatocytes

Given our findings of increased ATZ globule clearance as early as day 3 after BDL, corresponding to the period of acute liver injury, we investigated PASD co-staining with markers of cellular proliferation and apoptosis (Figure 2). In day 3 sham, Ki67+ cells are an infrequent but distinguishing feature of small clusters of repopulating GD hepatocytes, which is a typical finding in PiZZ mice (Figure 2A, left). In contrast, robust Ki67+ proliferative activity was observed in GD hepatocytes 3 days after BDL, in response to the acute liver injury (Figure 2A, right), and a very small subset of GC hepatocytes were Ki67+ (Figure 2C). Similarly, activated caspase-3 co-localized with GC hepatocytes in day 3 sham, but was surprisingly diminished 3 days after BDL (Figure 2B). These results suggest that regeneration of new GD hepatocytes may contribute to the “cleared” regions of GD cells; however, this turnover is not completely balanced by increased apoptosis of GC hepatocytes.

BDL induces increased expression of autophagic proteins in PiZZ mouse liver

Given our findings of increased proliferation of GD cells without comparable increase in apoptosis of GC cells, we hypothesized that the reduction in ATZ globules may involve intracellular protein clearance pathways rather than exclusively proliferation of new GD hepatocytes. Autophagy involves conjugation of Atg proteins and conversion of LC3I to LC3II. To further investigate possible intracellular mechanisms for ATZ globule clearance, we performed western blotting for members of the autophagy pathway, including beclin-1, Atg3, Atg7, Atg5, Atg12, Atg16L, and LC3A/B. BDL liver had increased expression of Atg5/12 (days 3 and 7; Figure 3A), and LC3A/B (days 3, 7, and 14; Figures 3A and 3B). These proteins signify later events in ubiquitin-like conjugation and the formation of autophagosomes. Specifically, Atg5 is an acceptor protein for the ubiquitin-like protein Atg12²² To further compare autophagic changes in GC and GD cells, we performed immunofluorescence microscopy for LC3 (green) and A1AT (red). As shown in Figure 3C and 3D, there was differential localization of LC3B in GD hepatocytes, compared to a very small subset of GC cells with A1AT globules. This suggests enhanced autophagy and protein clearance in GD hepatocytes after BDL.

BDL induces transcriptional reprogramming in PiZZ mouse liver

To further investigate altered gene expression pathways after BDL, we performed western blots on nuclear extracts for selected transcription factors known to regulate autophagy (Figure 4). As expected, increased nuclear FXR, a suppressor of autophagy, was observed early after BDL (Figure 4A), which appeared to trend down at later time points (Figure 4B)¹³. Surprisingly, nuclear TFEB, a master regulator of autophagy, was not significantly induced after BDL¹² Compared to wild-type and sham PiZZ mice, we did observe a significant decrease in nuclear C/EBP- α after BDL, while the expression of C/EBP- β appears to fluctuate. Both C/EBP isoforms are well-described regulators of liver regeneration²³.

Partial BDL induces localized ATZ globule clearance in PiZZ mouse liver

To determine if ATZ globule clearance was induced by retained bile acids versus systemic effects, we performed pBDL on PiZZ mice, where only the left bile duct was ligated; thus,

the unligated right lobe served as an internal control, subjected to the same dietary and systemic exposures as the left lobe. Although there was clear evidence of cholestasis in the ligated lobe after pBDL, serum biochemistries were less severely affected in pBDL mice (Figure 5A), confirming compensatory hepatic function from the unligated lobes. We then analyzed both ligated and unligated (control) lobes by globule morphometry, which again demonstrated approximately 50% reduction in ATZ globules in the ligated lobe compared to the unligated lobe (Figure 5B). Similar to total BDL, PASD stain (Figure 5C) confirmed large areas of clearing and bile ductular proliferation in the ligated lobe. These results confirm that localized retained bile acids have a direct microenvironmental stimulus on signaling pathways leading to ATZ globule clearance. Given that pBDL mice were overall healthier appearing with less severe lab abnormalities than BDL mice, systemic effects such as diet/starvation-induced autophagy, gut-liver axis, or other circulating factors are less likely causes for the dramatic reduction in globules.

Relationship of ATZ globule clearance to regeneration and autophagy in partial BDL

To identify mechanisms of ATZ globule clearance in the ligated lobe, we performed PASD co-staining for Ki67 and activated caspase 3 (Figure 6), as well as immunofluorescence staining for LC3B (Figure 7B). In pBDL, we observed Ki67+ proliferating GD hepatocytes (Figure 6A, right panel), as well as an absence of activated caspase-3 (Figure 6B, right panel) in the ligated lobe. We observed increased LC3B staining in the ligated lobe (Figure 7B, right panel) compared to the unligated lobe (Figure 7B, left panel), confirming increased autophagosome activity in GD cells. Coupled to our findings in total BDL, hepatocyte regeneration of GD cells appears to be an early response driven by local stimuli.

Differential expression of CYP-related genes in GC versus GD cells

To further investigate altered gene expression pathways in PiZZ mouse liver, we performed LCM on clusters of GC and GD hepatocytes, followed by gene array analysis. Interestingly, several genes involved in lipid metabolism, along with bile transport (Slc10a1), were upregulated in GD cells (Table 2). Surprisingly, CYP8b1, a key regulator of bile acid composition, was the second highest expressed gene in GD cells, with a 10.50-fold change over GC cells ($p=0.000338$). Increased expression was also noted for CYP2c54, CYP4a32, CYP2c50, CYP2c44, all of which are involved in arachidonic acid pathways. The complete gene array data set was deposited in NIH Gene Expression Omnibus (<http://www.ncbi.nlm.nih.gov/geo/>), accession ID# GSE84763.

Discussion

In summary, we found that retained bile acids trigger alternate transcriptional pathways and enhanced autophagy, leading to ATZ globule clearance in PiZZ mouse liver. Mice subjected to pBDL showed lobe-specific reduction in ATZ globules independent of dietary or systemic exposures, suggesting a localized effect when bile flow is obstructed. The increase in GD hepatocytes after BDL is an early regenerative response, coinciding with stimulation of proliferation, but not with increased apoptosis of GC hepatocytes. Overall, our data points to a hepatoprotective role for bile acids in A1ATD.

Numerous studies have reported the role of bile acid signaling in liver injury and protection. Elevated bile acids have been shown to accelerate liver regeneration²⁴. Bile acid composition has been used as a tool to assess graft function following liver transplantation²⁵⁻³⁰. Hydrophilic bile acids are cytoprotective. BDL in wild-type mice resulted in altered bile acid composition, with a significant increase in hydrophilic taurine-conjugated bile acids³¹. Similarly, the bile acid receptor TGR5 maintains hepatoprotective effects by limiting bile acid hydrophobicity³². In contrast, hydrophobic bile acids have been implicated in ER stress-induced apoptosis³³. In relation to this, we found CYP8b1 to be highly expressed in GD cells compared to GC cells, unlike in normal liver, where it is diffusely expressed³⁴. CYP8b1 catalyzes sterol hydroxylation, which in turn determines the ratio of primary bile acids and solubility³⁵. Whether such changes would affect the solubility of polymerized ATZ protein is not yet known, and our attempts to compare bile acid composition in BDL versus sham-operated PiZZ mice were unsuccessful due to technical issues.

Regulation of bile acid signaling also involves interaction of hepatic nuclear transcription factors, growth factors (FGF15/19), and bile acid receptors (FXR, TGR5) with the gut-liver axis^{11,13,32,36}. BDL also upregulates the nuclear transcription factor PPAR α ; although, the latter is not directly affected by bile acids. PPAR α is a master regulator of hepatic lipid metabolism³⁷. Furthermore, the nuclear receptors FXR and PPAR α both regulate autophagy, making these promising pharmacologic targets for enhancing ATZ clearance^{11,13}. It was recently reported that FXR suppresses autophagy by repressing CREB in the “fed” state, while PPAR α can reverse this suppression in the “fasted” state^{11,13}. Our analysis of key transcription factors after BDL (Figure 4) revealed several interesting findings. First, with increased exposure to retained bile acids after BDL, we observed down-trending of nuclear FXR, a transcription factor that acts as a bile acid receptor. Unfortunately, fasting in PiZZ mice can be lethal due to impaired glycogen stores³⁸. Since our mice were not fasted prior to sacrifice, our results do support FXR's role in suppressing autophagy¹³. Decreased FXR in the setting of BDL is intriguing, since that would in theory cause a decrease in SHP-1-mediated repression of CYP7a1 (cholesterol 7 α -hydroxylase), which catalyzes the first step of bile acid synthesis³⁹.

Given our findings of increased Atg5, Atg12, and LC3A/B after BDL (Figure 3), we were also surprised to see no increase in nuclear translocation of TFEB after BDL, as this transcription factor is a master regulator of autophagy. Cytoplasmic TFEB is dephosphorylated in the fasted state, and translocates to the nucleus to induce autophagy-related gene expression⁴⁰. TFEB gene transfer was previously shown to correct the liver disease in PiZZ mice, leading to increased degradation of polymerized ATZ in autolysosomes and decreased expression of ATZ monomers¹². Additional studies on PPAR α and other transcriptional regulators (mTORC1, NCoR1) may help to define the transcriptional program associated with autophagy in A1ATD.

Perhaps the most striking transcriptional change we observed was the fluctuation of both C/EBP- α and C/EBP- β isoforms after BDL (Figure 4), which is intriguing given the increased proliferation of GD hepatocytes. Normal liver regeneration following partial hepatectomy is regulated by the ratio of these two isoforms. During liver regeneration, C/EBP- β increases

and favors hepatocyte proliferation, while C/EBP- α decreases and has an opposing effect^{23,41}. C/EBP- α was recently shown in liver to be suppressed in conditions favoring autophagy and fibrosis⁴². Similar to our findings, Tao *et al.* found a reduction in hepatocyte C/EBP- α and an increase in Atg5 with autophagy⁴². Taken together, the C/EBP isoforms may represent novel regulators of autophagy; therefore, further investigation of hepatocyte regeneration in this setting are warranted.

In human liver, biliary obstruction activates cholangiocyte-associated transcription factors, and hepatocytes undergo gene expression reprogramming¹⁷. Thus, altered gene expression may be a common survival mechanism following BDL-induced liver injury. BDL causes cholestatic injury, ductular proliferation, and activation of liver progenitor cells in rodents⁴³. Our data supports those of Gao *et al.*, who recently found that in mice subjected to BDL, activation of autophagy in hepatocytes was protective against cholestatic liver injury¹⁵. It is interesting to note that our findings differ from a previous report of BDL in PiZZ mice⁴⁴. Brenner *et al.* found increased fibrosis, apoptosis, and stellate cell activation in PiZZ mouse liver after BDL. However, since their study focused on fibrosis as an endpoint, the mice were sacrificed 21 days after BDL, when more chronic severe liver injury was apparent. In contrast, we used earlier endpoints in our studies (days 3, 7, 14), to better characterize the dynamics of ATZ globule load and transcriptional changes. At these earlier time points, we observed increased ductular proliferation as expected, but little fibrosis.

In our experiments, the few remaining GC hepatocytes consistently resided adjacent to areas of proliferating bile ducts (Figures 1D, 5C, 7A). This is interesting, since developmentally ATZ globules first appear in peri-portal hepatocytes and then progress peri-centrally, and the pattern of globule clearance appears to be a reversal of this. Although the significance of this varied localization is unknown, it may represent active remodeling of the liver lobule in response to intercellular crosstalk.

Since the hepatic manifestations and clinical prognosis of A1ATD are highly variable, understanding these early changes after BDL may identify which factors predispose some patients to develop severe liver disease while sparing others. Although BDL is obviously not a viable option in patients, it does provide mechanistic clues for future investigation. Most children diagnosed with A1ATD present with neonatal cholestasis that peaks, but over time it spontaneously resolves without overt liver disease⁴⁵. Bile acid derivatives and their receptor agonists/antagonists are already in clinical development, and could potentially be repurposed for their autophagy-enhancing properties^{37,46}. Similarly, as a cytoprotective bile acid, ursodeoxycholic acid has been beneficial in children with mild-to-moderate A1ATD liver disease⁴⁷. Tauro-ursodeoxycholic acid also inhibited apoptosis induced by mutant ATZ protein⁴⁸. While our manuscript was in preparation, Tang *et al.* published that PiZZ mice treated with the exogenous bile acid nor-ursodeoxycholic acid showed a 32% increase in hepatic autophagy and >70% reduction of ATZ protein, with reduced apoptosis and liver injury⁴⁹. Our findings are consistent with those of Tang *et al.* and support comparable hepatoprotective effects. Clearly, a more focused approach to metabolomics and transcriptional regulation will offer a better understanding of A1ATD liver disease, so that novel therapeutic strategies can be tested.

Acknowledgments

We appreciate the excellent and generous technical assistance of Anne Orr, Meagan Haynes, John Stoops, Peng Zhang, Callen Wallace, Morgan Jessup, Mark Ross, Devin Boyles, and the Center for Biologic Imaging (Core A). We are grateful to Dr. David Geller for providing access to the Transplant/Microsurgery lab. Dr. Aaron Bell performed LCM with the assistance of Dr. Michael Ortell. Affymetrix analysis was performed by the Genomics Core, led by Dr. Jian-hua Luo. We also appreciate critical discussions with Dr. David Perlmutter and Dr. Sarangarajan Ranganathan.

Financial Support: ZK: K12HD052892, the Alpha-1 Foundation, the Hillman Foundation.

GKM, DBS, AWB: P01DK096990

References

1. Ghouse R, Chu A, Wang Y, Perlmutter DH. Mysteries of alpha1-antitrypsin deficiency: emerging therapeutic strategies for a challenging disease. *Dis Model Mech.* 2014; 7(4):411–9. [PubMed: 24719116]
2. Teckman JH, An JK, Blomenkamp K, Schmidt B, Perlmutter D. Mitochondrial autophagy and injury in the liver in alpha 1-antitrypsin deficiency. *Am J Physiol Gastrointest Liver Physiol.* 2004; 286(5):G851–62. [PubMed: 14684378]
3. Piitulainen E, Carlson J, Ohlsson K, Sveger T. Alpha1-antitrypsin deficiency in 26-year-old subjects: lung, liver, and protease/protease inhibitor studies. *Chest.* 2005; 128(4):2076–81. [PubMed: 16236857]
4. Sifers RN, Carlson JA, Clift SM, DeMayo FJ, Bullock DW, Woo SL. Tissue specific expression of the human alpha-1-antitrypsin gene in transgenic mice. *Nucleic Acids Res.* 1987; 15(4):1459–75. [PubMed: 3029716]
5. Khan Z. Pathogenesis of alpha-1 antitrypsin deficiency in the liver: New approaches to old questions. *J Liver Res Disord Ther.* 2016; 2(2):00023.
6. Lindblad D, Blomenkamp K, Teckman J. Alpha-1-antitrypsin mutant Z protein content in individual hepatocytes correlates with cell death in a mouse model. *Hepatology.* 2007; 46(4):1228–35. [PubMed: 17886264]
7. Hidvegi T, Ewing M, Hale P, Dippold C, Beckett C, Kemp C, Maurice N, Mukherjee A, Goldbach C, Watkins S, et al. An autophagy-enhancing drug promotes degradation of mutant alpha1-antitrypsin Z and reduces hepatic fibrosis. *Science.* 2010; 329(5988):229–32. [PubMed: 20522742]
8. Ding J, Yannam GR, Roy-Chowdhury N, Hidvegi T, Basma H, Rennard SI, Wong RJ, Avsar Y, Guha C, Perlmutter DH, et al. Spontaneous hepatic repopulation in transgenic mice expressing mutant human alpha1-antitrypsin by wild-type donor hepatocytes. *J Clin Invest.* 2011; 121(5):1930–4. [PubMed: 21505264]
9. Rudnick DA, Liao Y, An JK, Muglia LJ, Perlmutter DH, Teckman JH. Analyses of hepatocellular proliferation in a mouse model of alpha-1-antitrypsin deficiency. *Hepatology.* 2004; 39(4):1048–55. [PubMed: 15057909]
10. Pastore N, Blomenkamp K, Annunziata F, Piccolo P, Mithbaokar P, Maria Sepe R, Vetrini F, Palmer D, Ng P, Polishchuk E, et al. Gene transfer of master autophagy regulator TFEB results in clearance of toxic protein and correction of hepatic disease in alpha-1-anti-trypsin deficiency. *EMBO Mol Med.* 2013; 5(3):397–412. [PubMed: 23381957]
11. Lee JM, Wagner M, Xiao R, Kim KH, Feng D, Lazar MA, Moore DD. Nutrient-sensing nuclear receptors coordinate autophagy. *Nature.* 2014; 516(7529):112–5. [PubMed: 25383539]
12. Pastore N, Ballabio A, Brunetti-Pierri N. Autophagy master regulator TFEB induces clearance of toxic SERPINA1/alpha-1-antitrypsin polymers. *Autophagy.* 2013; 9(7):1094–6. [PubMed: 23584152]
13. Seok S, Fu T, Choi SE, Li Y, Zhu R, Kumar S, Sun X, Yoon G, Kang Y, Zhong W, et al. Transcriptional regulation of autophagy by an FXR-CREB axis. *Nature.* 2014; 516(7529):108–11. [PubMed: 25383523]
14. Asgharpour A, Kumar D, Sanyal A. Bile acids: emerging role in management of liver diseases. *Hepatol Int.* 2015; 9(4):527–33. [PubMed: 26320013]

15. Gao L, Lv G, Guo X, Jing Y, Han Z, Zhang S, Sun K, Li R, Yang Y, Wei L. Activation of autophagy protects against cholestasis-induced hepatic injury. *Cell Biosci.* 2014; 4:47. [PubMed: 25922659]
16. Manley S, Ni HM, Kong B, Apte U, Guo G, Ding WX. Suppression of autophagic flux by bile acids in hepatocytes. *Toxicol Sci.* 2014; 137(2):478–90. [PubMed: 24189133]
17. Limaye PB, Alarcon G, Walls AL, Nalesnik MA, Michalopoulos GK, Demetris AJ, Ochoa ER. Expression of specific hepatocyte and cholangiocyte transcription factors in human liver disease and embryonic development. *Lab Invest.* 2008; 88(8):865–72. [PubMed: 18574450]
18. Rudnick DA, Shikapwashya O, Blomenkamp K, Teckman JH. Indomethacin increases liver damage in a murine model of liver injury from alpha-1-antitrypsin deficiency. *Hepatology.* 2006; 44(4):976–82. [PubMed: 17006946]
19. Heinrich S, Georgiev P, Weber A, Vergopoulos A, Graf R, Clavien PA. Partial bile duct ligation in mice: a novel model of acute cholestasis. *Surgery.* 2011; 149(3):445–51. [PubMed: 20817234]
20. Khan Z, Michalopoulos GK, Stolz DB. Peroxisomal localization of hypoxia-inducible factors and hypoxia-inducible factor regulatory hydroxylases in primary rat hepatocytes exposed to hypoxia-reoxygenation. *Am J Pathol.* 2006; 169(4):1251–69. [PubMed: 17003483]
21. Vartak N, Damle-Vartak A, Richter B, Dirsch O, Dahmen U, Hammad S, Hengstler JG. Cholestasis-induced adaptive remodeling of interlobular bile ducts. *Hepatology.* 2016; 63(3):951–64. [PubMed: 26610202]
22. Romanov J, Walczak M, Ibricic I, Schuchner S, Ogris E, Kraft C, Martens S. Mechanism and functions of membrane binding by the Atg5-Atg12/Atg16 complex during autophagosome formation. *EMBO J.* 2012; 31(22):4304–17. [PubMed: 23064152]
23. Michalopoulos G. Terminating hepatocyte proliferation during liver regeneration: the roles of two members of the same family (CCAAT-enhancer-binding protein alpha and beta) with opposing actions. *Hepatology.* 2015; 61(1):32–4. [PubMed: 25066527]
24. Huang W, Ma K, Zhang J, Qatanani M, Cuvillier J, Liu J, Dong B, Huang X, Moore DD. Nuclear receptor-dependent bile acid signaling is required for normal liver regeneration. *Science.* 2006; 312(5771):233–6. [PubMed: 16614213]
25. Vilca Melendez H, Rela M, Setchell KD, Murphy GM, Heaton ND. Bile acids analysis: a tool to assess graft function in human liver transplantation. *Transpl Int.* 2004; 17(6):286–92. [PubMed: 15205724]
26. Ericzon BG, Eusufzai S, Kubota K, Einarsson K, Angelin B. Characteristics of biliary lipid metabolism after liver transplantation. *Hepatology.* 1990; 12(5):1222–8. [PubMed: 2227822]
27. Ericzon BG, Eusufzai S, Kubota K, Einarsson K, Angelin B. Biliary lipid secretion early after liver transplantation. *Transplant Proc.* 1990; 22(4):1537–8. [PubMed: 1975138]
28. Fujiwara S, Ku Y, Saitoh Y. Serum bile acid monitoring as an early indicator of allograft function in canine orthotopic liver transplantation. *Kobe J Med Sci.* 1992; 38(4):217–31. [PubMed: 1469887]
29. Hertl M, Harvey PR, Swanson PE, West DD, Howard TK, Shenoy S, Strasberg SM. Evidence of preservation injury to bile ducts by bile salts in the pig and its prevention by infusions of hydrophilic bile salts. *Hepatology.* 1995; 21(4):1130–7. [PubMed: 7705788]
30. Xu HS, Pilcher JA, Jones RS. Physiologic study of bile salt and lipid secretion in rats after liver transplantation. *Ann Surg.* 1993; 217(4):404–12. [PubMed: 8466312]
31. Zhang Y, Hong JY, Rockwell CE, Copple BL, Jaeschke H, Klaassen CD. Effect of bile duct ligation on bile acid composition in mouse serum and liver. *Liver Int.* 2012; 32(1):58–69. [PubMed: 22098667]
32. Pean N, Doignon I, Garcin I, Besnard A, Julien B, Liu B, Branchereau S, Spraul A, Guettier C, Humbert L, et al. The receptor TGR5 protects the liver from bile acid overload during liver regeneration in mice. *Hepatology.* 2013; 58(4):1451–60. [PubMed: 23686672]
33. Tamaki N, Hatano E, Taura K, Tada M, Kodama Y, Nitta T, Iwaisako K, Seo S, Nakajima A, Ikai I, et al. CHOP deficiency attenuates cholestasis-induced liver fibrosis by reduction of hepatocyte injury. *Am J Physiol Gastrointest Liver Physiol.* 2008; 294(2):G498–505. [PubMed: 18174271]

34. Wang J, Greene S, Eriksson LC, Rozell B, Reihner E, Einarsson C, Eggertsen G, Gafvels M. Human sterol 12 α -hydroxylase (CYP8B1) is mainly expressed in hepatocytes in a homogenous pattern. *Histochem Cell Biol*. 2005; 123(4-5):441–6. [PubMed: 15891895]
35. Gafvels M, Olin M, Chowdhary BP, Raudsepp T, Andersson U, Persson B, Jansson M, Bjorkhem I, Eggertsen G. Structure and chromosomal assignment of the sterol 12 α -hydroxylase gene (CYP8B1) in human and mouse: eukaryotic cytochrome P-450 gene devoid of introns. *Genomics*. 1999; 56(2):184–96. [PubMed: 10051404]
36. Naugler WE, Tarlow BD, Fedorov LM, Taylor M, Pelz C, Li B, Darnell J, Grompe M. Fibroblast Growth Factor Signaling Controls Liver Size in Mice With Humanized Livers. *Gastroenterology*. 2015
37. Rakhshandehroo M, Knoch B, Muller M, Kersten S. Peroxisome proliferator-activated receptor alpha target genes. *PPAR Res*. 2010; 2010
38. Hubner RH, Leopold PL, Kiuru M, De BP, Krause A, Crystal RG. Dysfunctional glycogen storage in a mouse model of alpha1-antitrypsin deficiency. *Am J Respir Cell Mol Biol*. 2009; 40(2):239–47. [PubMed: 18688041]
39. Goodwin B, Jones SA, Price RR, Watson MA, McKee DD, Moore LB, Galardi C, Wilson JG, Lewis MC, Roth ME, et al. A regulatory cascade of the nuclear receptors FXR, SHP-1, and LRH-1 represses bile acid biosynthesis. *Mol Cell*. 2000; 6(3):517–26. [PubMed: 11030332]
40. Settembre C, Zoncu R, Medina DL, Vetrini F, Erdin S, Erdin S, Huynh T, Ferron M, Karsenty G, Vellard MC, et al. A lysosome-to-nucleus signalling mechanism senses and regulates the lysosome via mTOR and TFE3. *EMBO J*. 2012; 31(5):1095–108. [PubMed: 22343943]
41. Jin J, Hong IH, Lewis K, Iakova P, Breaux M, Jiang Y, Sullivan E, Jawanmardi N, Timchenko L, Timchenko NA. Cooperation of C/EBP family proteins and chromatin remodeling proteins is essential for termination of liver regeneration. *Hepatology*. 2015; 61(1):315–25. [PubMed: 25043739]
42. Tao LL, Zhai YZ, Ding D, Yin WH, Liu XP, Yu GY. The role of C/EBP- α expression in human liver and liver fibrosis and its relationship with autophagy. *Int J Clin Exp Pathol*. 2015; 8(10):13102–7. [PubMed: 26722507]
43. Omori M, Everts RP, Omori N, Hu Z, Marsden ER, Thorgeirsson SS. Expression of alpha-fetoprotein and stem cell factor/c-kit system in bile duct ligated young rats. *Hepatology*. 1997; 25(5):1115–22. [PubMed: 9141427]
44. Mencin A, Seki E, Osawa Y, Kodama Y, De Minicis S, Knowles M, Brenner DA. Alpha-1 antitrypsin Z protein (PiZ) increases hepatic fibrosis in a murine model of cholestasis. *Hepatology*. 2007; 46(5):1443–52. [PubMed: 17668872]
45. Khan Z, Venkat VL, Soltys KA, Stolz DB, Ranganathan S. A Challenging Case of Severe Infantile Cholestasis in Alpha-1 Antitrypsin Deficiency. *Pediatr Dev Pathol*. 2016
46. Fiorucci S, Zampella A, Distrutti E. Development of FXR, PXR and CAR agonists and antagonists for treatment of liver disorders. *Curr Top Med Chem*. 2012; 12(6):605–24. [PubMed: 22242859]
47. Lykavieris P, Ducot B, Lachaux A, Dabadie A, Broue P, Sarles J, Bernard O, Jacquemin E. Liver disease associated with ZZ alpha1-antitrypsin deficiency and ursodeoxycholic acid therapy in children. *J Pediatr Gastroenterol Nutr*. 2008; 47(5):623–9. [PubMed: 18955864]
48. Miller SD, Greene CM, McLean C, Lawless MW, Taggart CC, O'Neill SJ, McElvaney NG. Tauroursodeoxycholic acid inhibits apoptosis induced by Z alpha-1 antitrypsin via inhibition of Bad. *Hepatology*. 2007; 46(2):496–503. [PubMed: 17559149]
49. Tang Y, Fickert P, Trauner M, Marcus N, Blomenkamp K, Teckman J. Autophagy induced by exogenous bile acids is therapeutic in a model of alpha-1-AT deficiency liver disease. *Am J Physiol Gastrointest Liver Physiol*. 2016; 311(1):G156–65. [PubMed: 27102560]

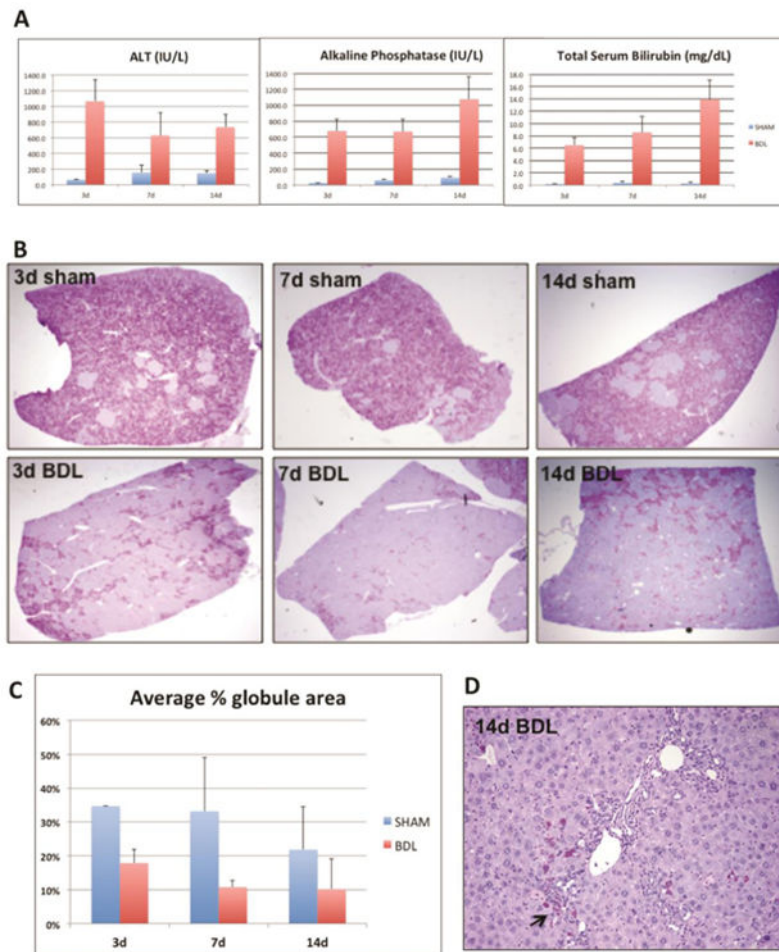


Figure 1. Bile duct ligation induces clearance of ATZ globules in PiZZ mouse liver

A. Serum ALT, alkaline phosphatase, and total bilirubin levels at days 3, 7, and 14 after BDL or sham operations. B. Low power views of PASD stains show dramatic clearance of ATZ globules from the liver lobe (40× magnification). C. Quantitative results of ATZ globule morphometry showing percent of PASD globules present in the tissue section. D. PASD stain showing “cleared” region after 14d BDL (100× magnification). Arrow points to residual GC hepatocytes intermixed within areas of ductal proliferation.

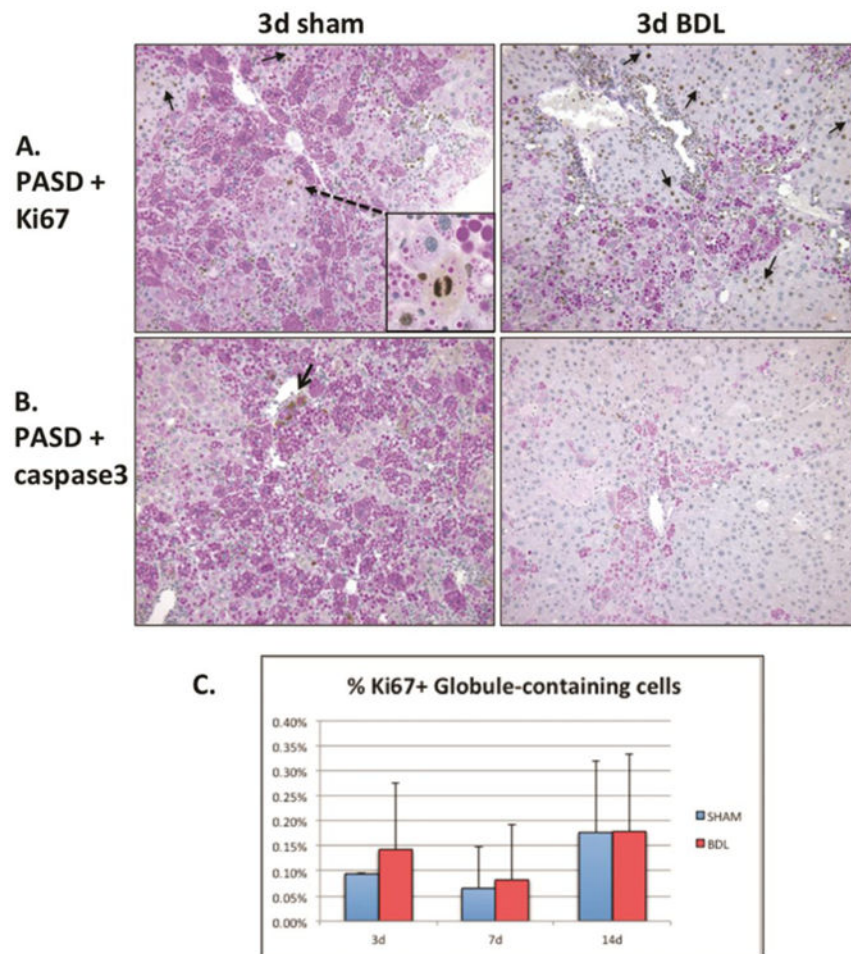


Figure 2. Bile duct ligation induces an early regenerative response in GD hepatocytes 3 days after surgery

A. Ki67 immunohistochemistry co-stained with PASD shows regenerating Ki67+ GD hepatocytes (arrows). Inset shows a rare mitosis within a repopulating cluster of GD cells in sham control. B. Activated caspase-3 immunohistochemistry co-stained with PASD does not show significant apoptosis in GC hepatocytes after BDL (200× magnification). C. Quantitative immunofluorescence data for the cell proliferation marker Ki67 and anti-human A1AT. Graph depicts a small subset of %Ki67+ cells co-localizing with ATZ globule-containing cells (normalized to total # of cells).

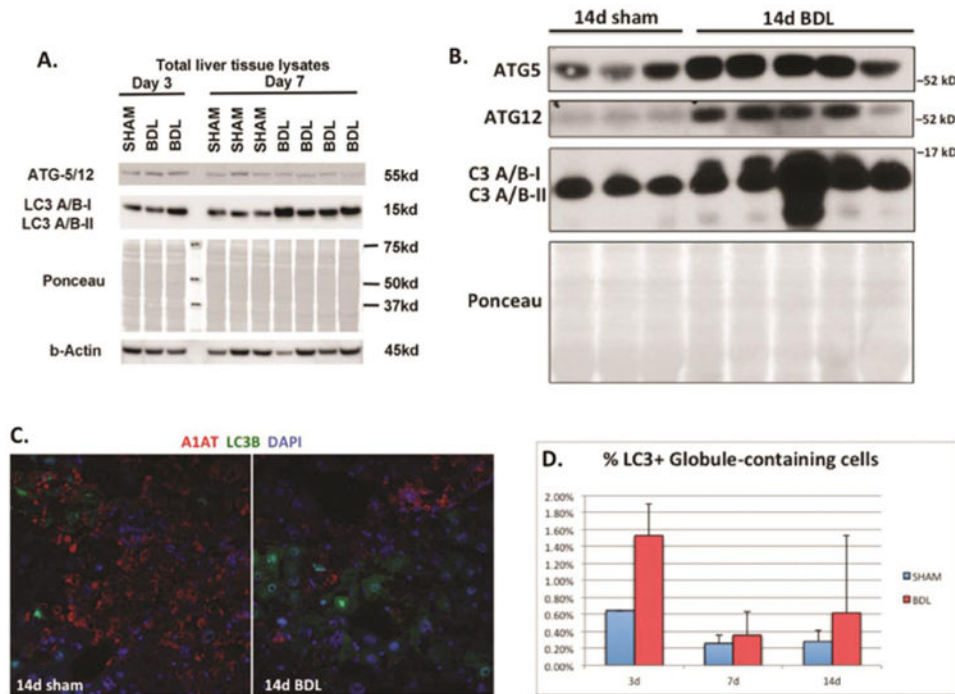


Figure 3. Bile duct ligation induces increased expression of autophagic proteins in PiZZ mouse liver

A and B. Western blots of total liver tissue lysates showing increased Atg5, Atg12, and LC3A/B after BDL compared to sham livers. Ponceau is shown to confirm equal loading, since cytoskeletal changes can affect both actin and tubulin in PiZZ mouse liver. C. Confocal immunofluorescence microscopy showing the majority of LC3B (green) does not co-localize with GC cells labeled with anti-human A1AT (red) antibody (100× magnification). D. Quantitative immunofluorescence data for the LC3 and anti-human A1AT. Graph depicts a small subset of %LC3+ cells co-localizing with ATZ globule-containing cells (normalized to total # of cells).

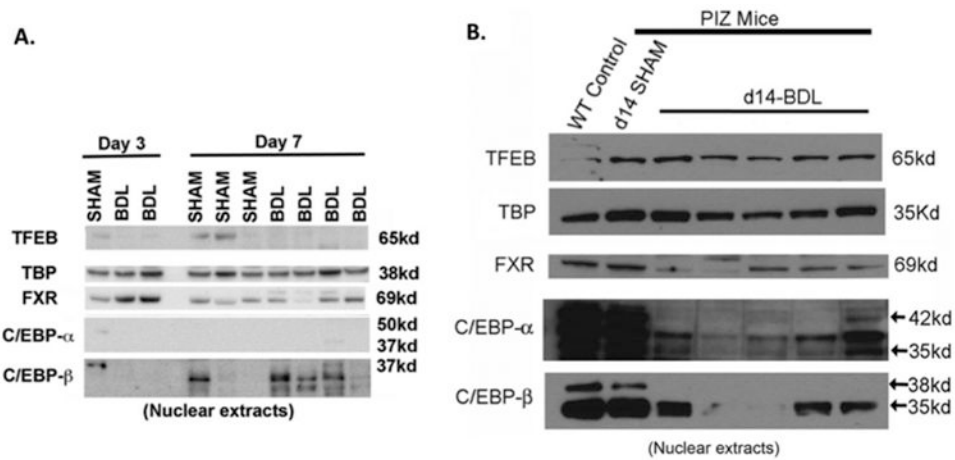


Figure 4. Bile duct ligation induces transcriptional reprogramming in PiZZ mouse liver
 A. and B. Western blot of nuclear proteins showing decreased nuclear C/EBP- α and C/EBP- β isoforms in BDL livers compared to sham-operated and wild-type (WT) control liver. Nuclear FXR is decreased after BDL at later time points. Nuclear TFEB is not significantly changed in BDL and sham livers. TATA-binding protein (TBP) serves as the nuclear protein loading control.

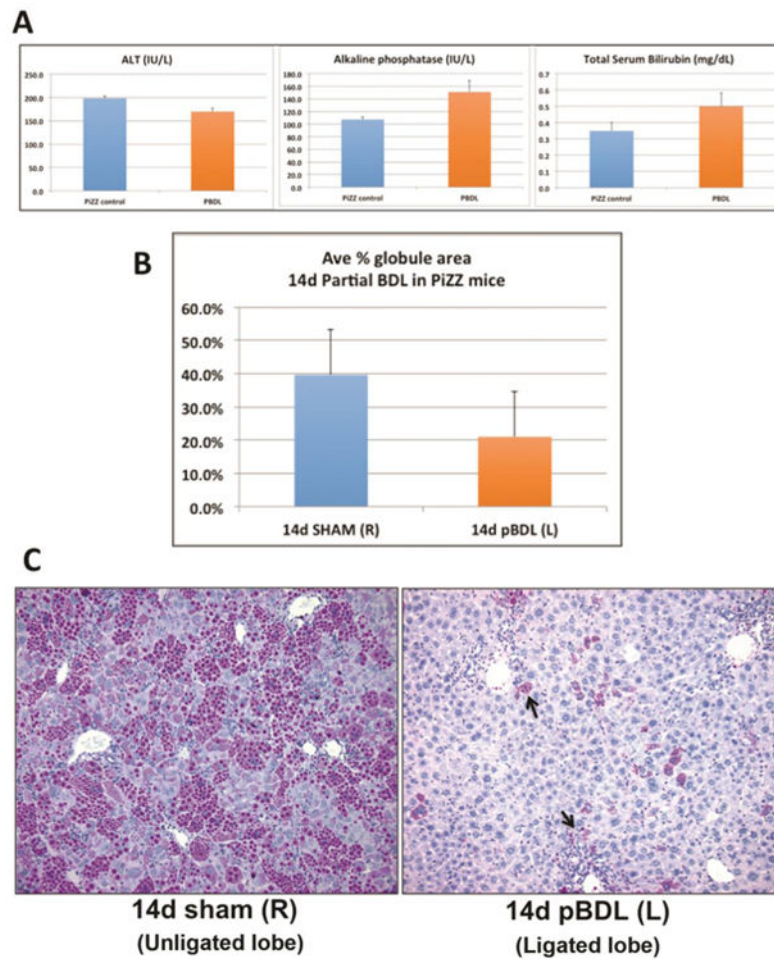


Figure 5. Partial bile duct ligation induces localized ATZ globule clearance in PiZZ mouse liver
 A. Serum ALT, alkaline phosphatase, and total bilirubin levels in mice 14 days after pBDL are comparable to age- and sex-matched unoperated PiZZ (control) mice. As expected, biochemical parameters in BDL mice (shown in Figure 1A) are significantly worse compared to pBDL values. B. Quantitative results of ATZ globule morphometry showing decreased percentage of PASD globules present in the ligated left lobe (pBDL) compared to the unligated right control lobe. C. PASD staining showing the cleared areas of ATZ globules in pBDL (ligated left lobe, right panel) compared to control (unligated right lobe, left panel). Arrows point to residual GC hepatocytes intermixed within areas of ductal proliferation, similar to total BDL (200 \times magnification).

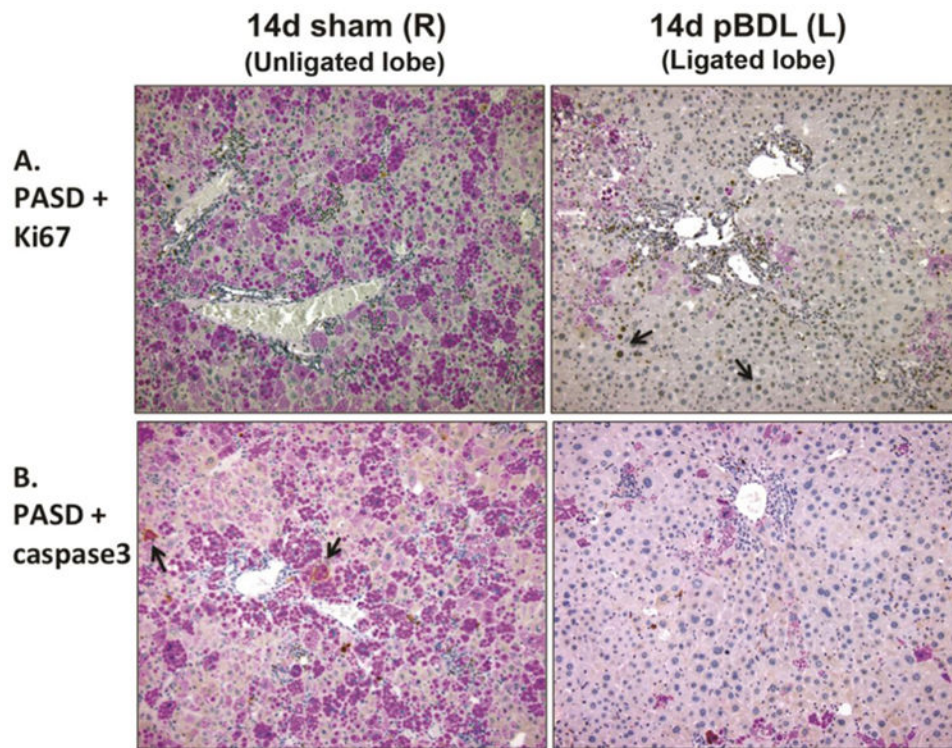


Figure 6. Relationship of ATZ globule clearance to regeneration in partial bile duct ligation
 A. Ki67 immunohistochemistry co-stained with PASD shows persistence of regenerating Ki67+ GD hepatocytes 14 days after pBDL (right panel, arrows). B. Activated caspase-3 immunohistochemistry co-stained with PASD does not show significant apoptosis in GC hepatocytes 14 days after pBDL (right panel), compared to unligated right control lobe (left panel, arrows; 200× magnification).

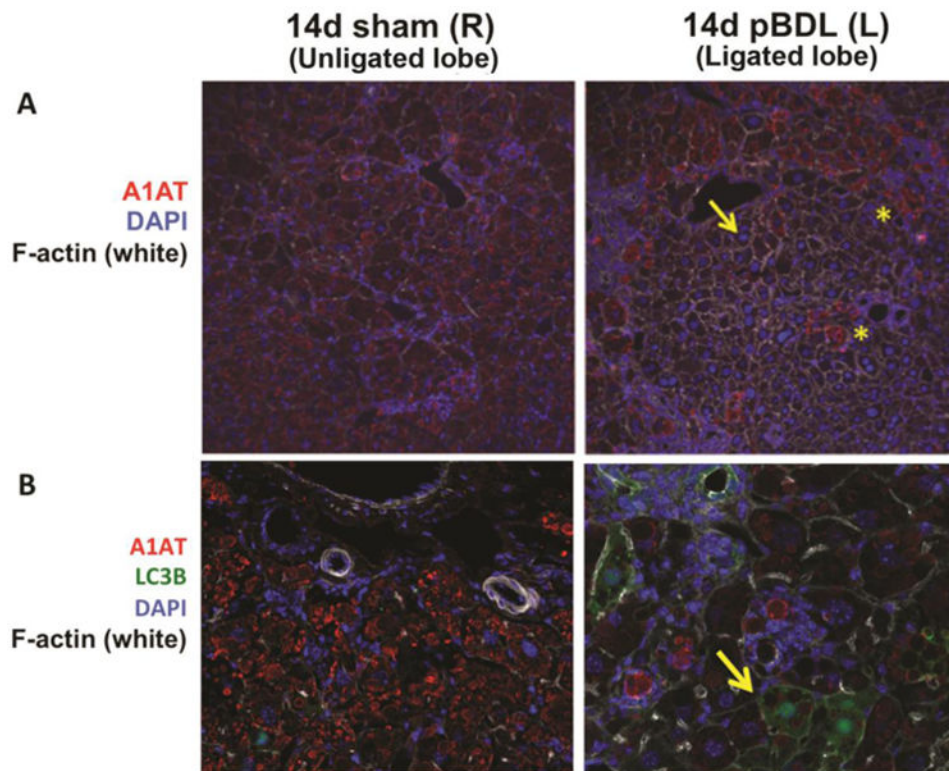


Figure 7. Relationship of ATZ globule clearance to autophagy in partial bile duct ligation
 A. Confocal immunofluorescence microscopy showing the cleared areas of red ATZ globules in pBDL lobe (right panel, arrow) compared to unligated control lobe (left panel). Asterisks (*) point to residual GC hepatocytes intermixed within areas of ductal proliferation (100× magnification). B. Increased LC3B staining (green, right panel, arrow) in GD hepatocytes in the ligated pBDL lobe (200× magnification).

Table 1
List of antibodies used in this study

Antibody	Clone (Source)	Dilution	Method
A1AT	Goat pAb #A80-122A (Bethyl)	1:1000	IF
ATG5	Rabbit mAb D5F5U (Cell Signaling)	1:1000	WB
ATG12	Rabbit mAb D888H11 (Cell Signaling)	1:1000	WB
Activated Caspase-3	Rabbit pAb #9661 (Cell Signaling)	1:200	IHC
C/EBP- α	Rabbit pAb 14AA (Santa Cruz)	1:1000	WB
C/EBP- β	Rabbit pAb C-19 (Santa Cruz)	1:1000	WB
LC3A/B	Rabbit mAb D3U4C (Cell Signaling)	1:1000	WB
LC3B	Rabbit pAb #NB100-2220 (Novus Biologicals)	1:200	IF
Ki67	Rabbit mAb SP6 (ThermoFisher)	1:50	IHC
TBP	Mouse mAb 1TBP18 (Abcam)	1:200	WB
TFEB	Goat pAb V-17 (Santa Cruz)	1:1000	WB

IF = immunofluorescence, IHC = immunohistochemistry, mAb = monoclonal, pAb = polyclonal, WB = western blot

Table 2
Differential expression of bile related-genes in microdissected PiZZ mouse liver

Fold (GD/GC)	Gene ID	Gene name
10.50	Cyp8b1	cytochrome P450, family 8, subfamily b, polypeptide 1
5.79	Cyp2c54	cytochrome P450, family 2, subfamily c, polypeptide 54
4.66	Cyp4a32	cytochrome P450, family 4, subfamily a, polypeptide 32
4.65	Cyp2c50	cytochrome P450, family 2, subfamily c, polypeptide 50
4.32	Cyp2c44	cytochrome P450, family 2, subfamily c, polypeptide 44
4.08	Slc10a1	solute carrier family 10 (sodium/bile acid cotransporter family), member 1
3.60	Cyp2c37	cytochrome P450, family 2, subfamily c, polypeptide 37
3.23	Cyp4a10	cytochrome P450, family 4, subfamily a, polypeptide 10
3.21	Cyp2f2	cytochrome P450, family 2, subfamily f, polypeptide 2
3.03	Cyp4a14	cytochrome P450, family 4, subfamily a, polypeptide 14
2.49	Cyp4a31	cytochrome P450, family 4, subfamily a, polypeptide 31
2.23	Cyp4f15	cytochrome P450, family 4, subfamily f, polypeptide 15
1.97	Cyp2j9	cytochrome P450, family 2, subfamily j, polypeptide 9
1.94	Cyp2d13	cytochrome P450, family 2, subfamily d, polypeptide 13;
1.90	Cyp2c68	cytochrome P450, family 2, subfamily c, polypeptide 68
1.89	Cyp7b1	cytochrome P450, family 7, subfamily b, polypeptide 1
1.74	Cyp2j5	cytochrome P450, family 2, subfamily j, polypeptide 5
1.70	Cyp26a1	cytochrome P450, family 26, subfamily a, polypeptide 1
1.70	Cyp2c67	cytochrome P450, family 2, subfamily c, polypeptide 67
1.68	Klkb1; Cyp4v3	kallikrein B, plasma 1; cytochrome P450, family 4, subfamily v, polypeptide 3
1.67	Cyp2u1	cytochrome P450, family 2, subfamily u, polypeptide 1
1.63	Cyp2d40	cytochrome P450, family 2, subfamily d, polypeptide 40
1.61	Cyp3a13	cytochrome P450, family 3, subfamily a, polypeptide 13
1.60	Cyp2d26	cytochrome P450, family 2, subfamily d, polypeptide 26
1.59	Cyp2d22	cytochrome P450, family 2, subfamily d, polypeptide 22
1.57	Cyp4f14	cytochrome P450, family 4, subfamily f, polypeptide 14
1.57	Cyp2c40	Cytochrome P450, family 2, subfamily c, polypeptide 40
1.56	Cyp39a1	cytochrome P450, family 39, subfamily a, polypeptide 1
1.54	Cyp2a12	cytochrome P450, family 2, subfamily a, polypeptide 12
1.52	Cyp2c69	cytochrome P450, family 2, subfamily c, polypeptide 69
1.41	Cyp2g1	cytochrome P450, family 2, subfamily g, polypeptide 1
1.48	Slc10a5	solute carrier family 10 (sodium/bile acid cotransporter family), member 5